Role of the Charged Groups of Glutathione Disulfide in the Catalysis of Glutathione Reductase: Crystallographic and Kinetic Studies with Synthetic Analogues†

Wolfgang Janes and Georg E. Schulz*
Institut für Organische Chemie und Biochemie der Universität, Albertstrasse 21, 7800 Freiburg i.Br., West Germany
Received October 2, 1989; Revised Manuscript Received December 26, 1989

ABSTRACT: Six analogues of glutathione disulfide were synthesized. All of them involved the abolishment of charges, either by amidation of carboxylates or by removal of amino groups. Four of these analogues could be bound to crystalline oxidized glutathione reductase, and their binding modes could be established by X-ray analyses at 2.4-Å resolution. All six analogues were catalytically processed; the kinetic parameters were determined. The two analogues that did not bind in the crystals had by far the poorest catalytic efficiencies. Kinetic parameters together with X-ray data show the influence of each charged group on binding and catalytic rate. Data analysis indicates that the enzyme avoids processing of incorrect substrates in two ways: First, it reduces their binding strengths and/or enforces displacement of catalytically important substrate parts. Furthermore, it forms a fragile cluster of bound substrate and catalytically competent residues, which is unbalanced by incorrect parts of the substrate such that catalysis is prevented. A scouting microcalorimetric study using glutathione disulfide yielded a binding enthalpy of −103 (±10) kJ/mol at 25 °C and a heat capacity change of −8 (±1) kJ·mol^{-1}·K^{-1}. The study showed that it is feasible to measure these parameters as a function of substrate modification.

To perform rational drug design on enzymes [e.g., Hol (1986)], the structures of enzyme/ligand complexes and also the contribution of individual atomic groups to binding and catalysis have to be known. If crystal structure analyses are at 2-Å resolution or better, hydrogen bonds are accurate enough to allow a strength estimate (Baker & Hubbard, 1984). Furthermore, crystallographic temperature factors are then well enough known to differentiate between more or less rigidly fixed atomic groups (Holden & Matthews, 1988; Karplus & Schulz, 1989). More detailed information on the roles of particular atomic groups is obtained if synthetic substrate analogues containing slight modifications at these groups are correlated to binding and catalysis.

Here, we are concerned with the glutathione system. Reduced glutathione (GSH)[1] fulfills numerous metabolic roles as has been reviewed recently (Dolphin et al., 1989). In many of these functions it is oxidized to glutathione disulfide (GSSG), which is then recycled to GSH by the reaction GSSG + NADPH + H$^+$ ⇌ 2 GSH + NADP$^+$ catalyzed by the intracellular enzyme glutathione reductase (GR, EC 1.6.4.2, homodimer M_r = 104 800). GR is a potent drug target and therefore of appreciable medical interest (Schirmer et al., 1989). The structures of GR and of its complexes with both substrates are well-known at resolutions better than 2 Å (Karplus & Schulz, 1989). The catalytic reaction is elucidated in mechanistic detail (Sustmann et al., 1989). To establish the roles of particular atomic groups of the substrate, we have now analyzed binding and catalysis of GSSG analogues carrying small modifications. Furthermore, a microcalorimetric measurement with GSSG showed that this analysis can be extended to thermodynamic parameters.

Materials and Methods

The GSSG analogues were synthesized in milligram amounts by using the mixed anhydride method (Wieland & Sieber, 1969). The synthesized compounds and their abbreviations are given in Figure 1. The correct structure and the purity of each intermediate was established by elemental analysis, thin-layer chromatography, and ^{1}H NMR (Bruker, 250 MHz). The homogeneity of the final products was checked by ^{1}H NMR, HPLC, and thin-layer electrophoresis. Details of the procedures will be published elsewhere. The analogues were subjected to a quantitative amino acid analysis, which has an accuracy of about ±10% (Williams, 1986). This accuracy refers to all given analogue concentrations. The enzyme GR was taken from human erythrocytes. Following the procedure of Krohne-Ehrich et al. (1977) it was isolated from outdated blood reserves kindly provided by the Wehrmedizinisches Institut, Koblenz.

For X-ray structure analyses of the enzyme/ligand complexes, GR was crystallized in form B (Thieme et al., 1981). The enzyme crystals were then soaked with GSSG analogues dissolved in crystal handling buffer at 20 °C (Table I). This buffer was 0.1 M phosphate (potassium salt) and 2 M ammonium sulfate, pH 6.9 at 20 °C. The crystals were mounted by using the soaking solution. X-ray data were collected on a four-circle diffractometer (Nicolet, modified Model P2$_1$) in one to five radial shells using Ni-filtered Cu Kα radiation. To reduce radiation damage, all measurements were done at 6 °C. For data reduction we followed the procedure of Thieme et al. (1981). Typical crystal sizes and ω scan rates and widths were 900·500·400 μm^3, 0.8 deg/min and 0.5°, respectively.

All data were initially evaluated with $(F_{soak} - F_{nat})\exp i\alpha_{calc}$ difference Fourier maps, where F_{nat} values are the observed structure factor amplitudes of the native crystals and α_{calc} values are the calculated phases of the native crystals as established in a refinement at 1.54-Å resolution (Karplus & Schulz, 1987). The four GSSG analogues that bound in the crystal were modeled into the difference Fourier maps by using

† This work was supported by the Deutsche Forschungsgemeinschaft.

[1] Abbreviations: GR, glutathione reductase; GSH, glutathione; GSSG, glutathione disulfide; sGa, bGa, sEa, bEa, sdE, bdE, analogues of GSSG (see Figure 1); EDTA, ethylenediaminetetraacetate.

0006-2960/90/0429-4022$02.50/0

Table I: X-ray Structure Analyses of Crystalline GR/GSSG Analogue Complexes

GSSG analogue (abbrev)	soaking conditions: concn (mM)	soaking conditions: time (days)	resolution (Å)	R_{int}[a,b] (%)	R_{nat}[a,b] (%)	R_{mod}[a] (%)	rel[c] occupancy (%)	modified group of bound GSSG analogue
semi-Gly-amide (sGa)	10	0.7	2.4	3.9	8.0	16.1	100	Gly-II carboxylate
bis-Gly-amide (bGa)	10	17	2.4	5.8	7.4	15.1	80	Gly-II and Gly-I carboxylates
semi-Glu-amide (sEa)	20	0.7	2.4	2.8	5.8	15.1	80[d]	Glu-I carboxylate
bis-Glu-amide (bEa)	20	0.7	5.9	5.4	5.8		0	Glu-I and Glu-II carboxylates
semi-deamino-Glu (sdE)	20	0.7	2.4	2.2	7.2	14.6	100	Glu-I amino
bis-deamino-Glu (bdE)	20	0.6	3.0	2.5	7.0		low[e]	Glu-I and Glu-II aminos

[a] The R factors are defined as $R = 2\sum|F_1 - F_2|/\sum(F_1 + F_2)$, where the data sets 1 & 2 are symmetry-related reflections for R_{int}, $F_{soak(obs)}$ & $F_{native(obs)}$ for R_{nat}, and $F_{soak(obs)}$ & $F_{calc(liganded)}$ for R_{mod}. [b] Only the resolution range ∞ to 5.9 Å is taken into account. [c] See text; 100% relative occupancy corresponds to an absolute occupancy between 40% and 80%. [d] The highest difference density was at Cys284. [e] Only low densities at Glu-II and Cys-II were visible. The highest difference densities were at His75 and His82.

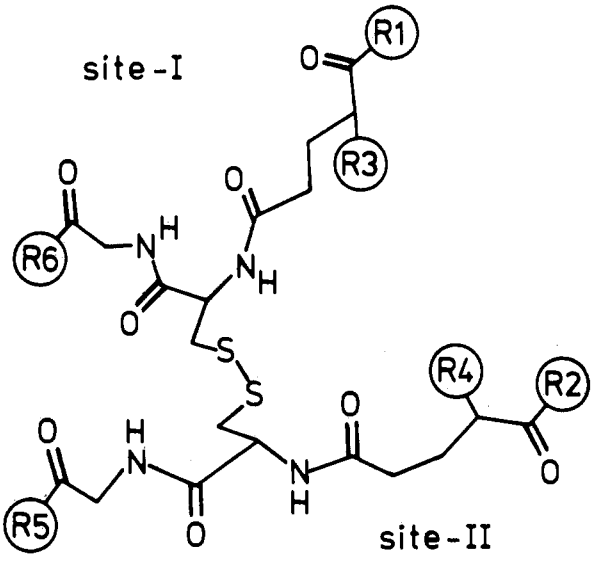

R1	R2	R3	R4	R5	R6	NAME
OH	OH	NH_2	NH_2	OH	OH	GSSG
OH	OH	NH_2	NH_2	NH_2	OH	semi-Gly-amide , sGa
OH	OH	NH_2	NH_2	NH_2	NH_2	bis-Gly-amide , bGa
NH_2	OH	NH_2	NH_2	OH	OH	semi-Glu-amide , sEa
NH_2	NH_2	NH_2	NH_2	OH	OH	bis-Glu-amide , bEa
OH	OH	H	NH_2	OH	OH	semi-deamino-Glu, sdE
OH	OH	H	H	OH	OH	bis-deamino-Glu, bdE

FIGURE 1: Scheme of the modifications of glutathione disulfide together with the names and abbreviations used in the text. To facilitate comparisons, GSSG is depicted in the same conformation and view as in Figure 6. One should keep in mind that the covalent structure of GSSG is symmetrical, while the spatial structure of GSSG as bound to GR is asymmetrical. Residues bound at a particular site are named accordingly (e.g., Glu-I, Gly-II). In anticipation of the results of this work, the labels of the modified groups are arranged to agree with the enzyme-bound GSSG analogues; e.g., the carboxamide of sEa is at site I.

the program FRODO (Jones, 1978) on a stereo color vector display (Evans & Sutherland, Model PS-330). Model building started always with the GSSG model derived from the GR/GSSG complex (Karplus & Schulz, 1989). Usually, only slight modifications were necessary. The model coordinates were refined with the TNT program package of Tronrud et al. (1987) using the final weights (geometry vs X-ray data) from the 1.54-Å refinement of native GR. Atomic temperature factors and occupanices of protein with solvent were taken from the refined native enzyme. The 14 solvent molecules displaced by GSSG in the GR/GSSG complex were deleted. For the ligands, all occupancies were set to 100%, and the temperature factors were taken from the GR/GSSG complex. All occupancies and temperature factors were kept fixed. At 2.4-Å resolution they cannot be refined separately. Also, we restrained from fixing the temperature factors to refine the occupancies, because the temperature factors of the analogues differed obviously from each other and from those of GSSG, rendering any resulting occupancy inconclusive. The final deviations of the models from standard geometries were 0.03 Å in bond lengths and 3° in bond angles. Further details are given in Table I.

For measuring enzyme activities we followed the oxidation of NADPH at 366 nm (Eppendorf, Model 1100 M) in a direct spectrophotometric assay (Worthington & Rosemeyer, 1974). The assay buffer was 50 mM phosphate (potassium salt), 200 mM KCl, and 1 mM EDTA at pH 6.9. We added 10 μL of NADPH (20 mM in buffer) and 1–100 μL of substrate (GSSG analogue in buffer) to 500 μL of buffer. After thermal equilibration at 25 °C, the reaction was started by the addition of enzyme dissolved in 10 μL of buffer. The amounts of enzyme and the used concentrations of the GSSG analogues and GSSG are given in Table II. For GSSG and four analogues, we derived V_{max} and K_m values from double-reciprocal plots. For two analogues, only V_{max}/K_m ratios could be derived from direct plots.

In a scouting experiment we measured the binding enthalpy of the nonproductive complex between GSSG and the oxidized enzyme as a function of temperature with a microcalorimeter (LKB, Model 10700). For this purpose we prepared a buffer containing 100 mM phosphate (potassium salt), 200 mM KCl, and 1 mM EDTA, pH 7.0 at 20 °C. Two 2-mL aliquots of 20 mM GSSG in this buffer were applied to the reservoirs of the reaction and the reference cells, respectively. Furthermore, 4 mL of 61 μM (active sites, 3.2 mg/mL protein, see Table II) enzyme in this buffer was placed into the main chamber of the reaction cell and 4 mL of buffer into the main chamber of the reference cell. The microcalorimeter was equilibrated overnight at five different temperatures in the range 20–40 °C. The binding enthalpy was measured as the integral over a transient temperature difference between the cells arising on mixing reservoirs and main chambers. Conversion to energies was done with defined electric heat pulses.

RESULTS

Binding of GSSG Analogues in the Crystal. Crystals were mostly soaked overnight (Table I). Data were first collected to 5.9-Å resolution and analyzed by difference Fourier maps. Clear binding at the GSSG site occurred with the analogues sGa, bGa, sEa, and sdE; no density at all was observed for bEa in two independent experiments. This is in agreement with the $R_{nat} - R_{int}$ differences of Table I. For bdE, the $R_{nat} - R_{int}$ difference indicates binding, but the difference Fourier maps

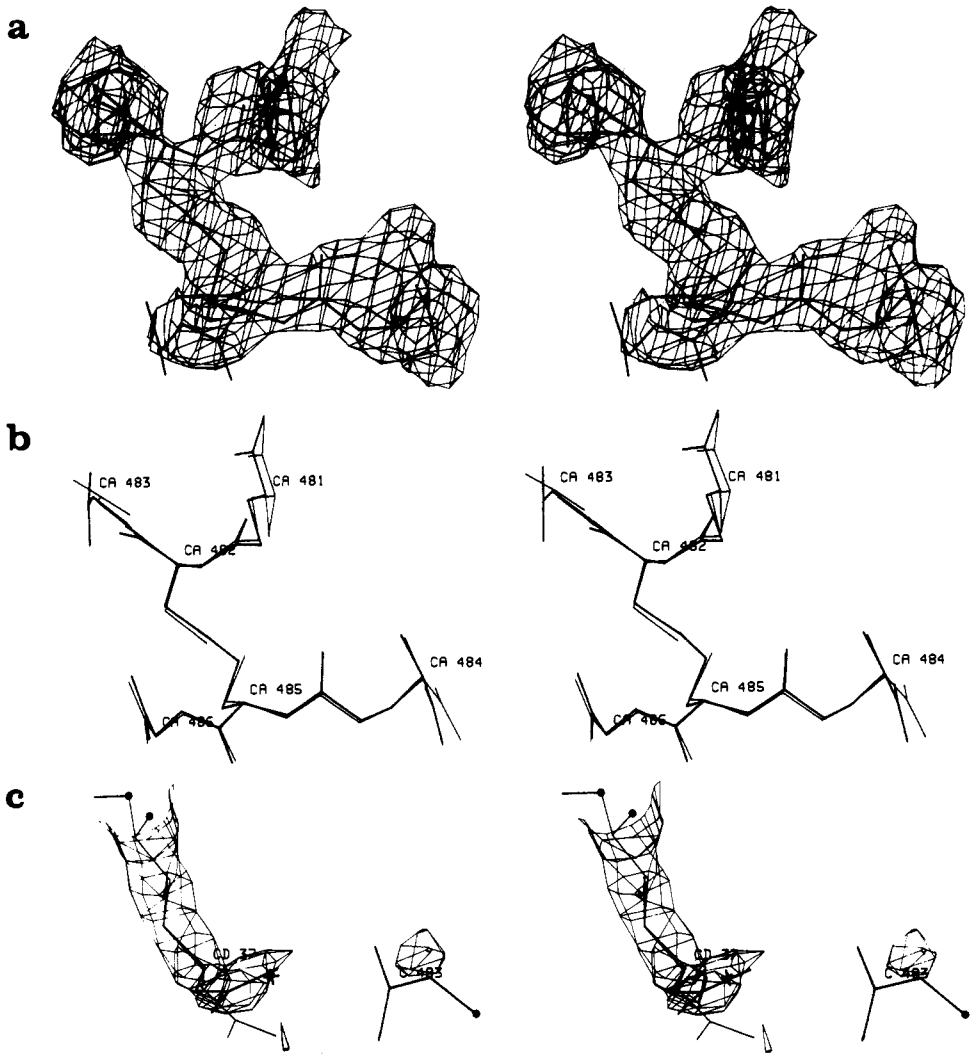

FIGURE 2: Structural analysis of the GSSG analogue bis-Gly-amide (bGa) as bound to crystalline glutathione reductase. (a) Difference Fourier electron density map with the refined model of bGa; the cut level is at 20% of maximum density (=1.5σ, where σ is the root mean square electron density of the map). (b) Overlay of refined model of bGa (thick lines) with GSSG [thin lines, disulfide not connected; taken from Karplus and Schulz (1989)]. Residue numbers 481–486 refer to Glu-I, Cys-I, Gly-I, Glu-II, Cys-II, and Gly-II of enzyme-bound GSSG, respectively. (c) Additive Fourier electron density map ($2F_{soak} - F_{nat}$) exp$i\alpha_{calc}$ showing the refined models of Gly-I of bGa and Arg37 (thick lines). Arg37 corresponds to the native conformation. The Arg37 conformation with bound GSSG is given as thin lines. The cut level is at 15% of maximum density (=1.4σ). Chain cuts are marked by dots. The cross represents a solvent molecule.

at 5.9- and 3-Å resolution had only weak density around sites Glu-II and Cys-II of the GSSG site showing low, local occupancy. Model building was not possible. Stronger positive and negative densities of small volumes occurred at His75 and His82 far away from the GSSG site. A closer inspection of these densities showed that His75 and His82, which are located between the internal cavity of GR and the intersubunit disulfide Cys90:Cys90′ (Karplus & Schulz, 1987), were shifted by about 1 Å from the cavity toward the disulfide. Such a shift could be caused by (disordered) ligand binding in the cavity. The difference electron density map showed also a movement of the catalytic team at His467′, which was similar to the shift observed with sdE (see below). The soaking conditions for bdE were appropriate, since similar weak binding had been observed (Scheuring, 1988) with a shorter soak (2 h) at lower bdE concentration (6.7 mM).

For sGa, bGa, sEa, and sdE the data collection was extended to 2.4-Å resolution by using a single crystal and measuring about 21 000 reflections for each analogue. The average radiation damage was around 8%. At this resolution the difference densities sufficed to build models for all four analogues. While for sGa, bGa, and sdE the major difference density was at the GSSG site, the highest difference density of sEa was found at Cys284 at the protein surface far away from the GSSG site and also from His75 and His82. This density was 15% higher than the density at the GSSG site but smaller than the volume of a single amino acid residue. It is remarkable that at Cys284 as well as at the cavity close to His75 and His82 strong structural changes with noninterpretable additional densities had also been observed with other GSSG analogues (Bilzer et al., 1984; Karplus et al., 1989).

Binding of bGa. The observed difference density of bGa is depicted in Figure 2a. The model could easily be built following the GR/GSSG complex. Since both glycines are amidated in bGa, no ambiguity between a carboxylate and a carboxamide had to be resolved. The difference density accounts for all features of the model except for Gly-II, which binds also poorly with GSSG (Karplus & Schulz, 1989) and with the other analogues (see Figures 3a, 4a, and 5a). After coordinate refinement, the model of bGa was compared with GSSG (Figure 2b). Except for Gly-I, both models agree with each other within the limits of the coordinate error, which is estimated to be about 0.3 Å.

At Gly-I the carboxamide is shifted by 0.5 Å and rotated by 40° in relation to the carboxylate of GSSG. On bGa binding, the guanidinium group of Arg37, which is the direct

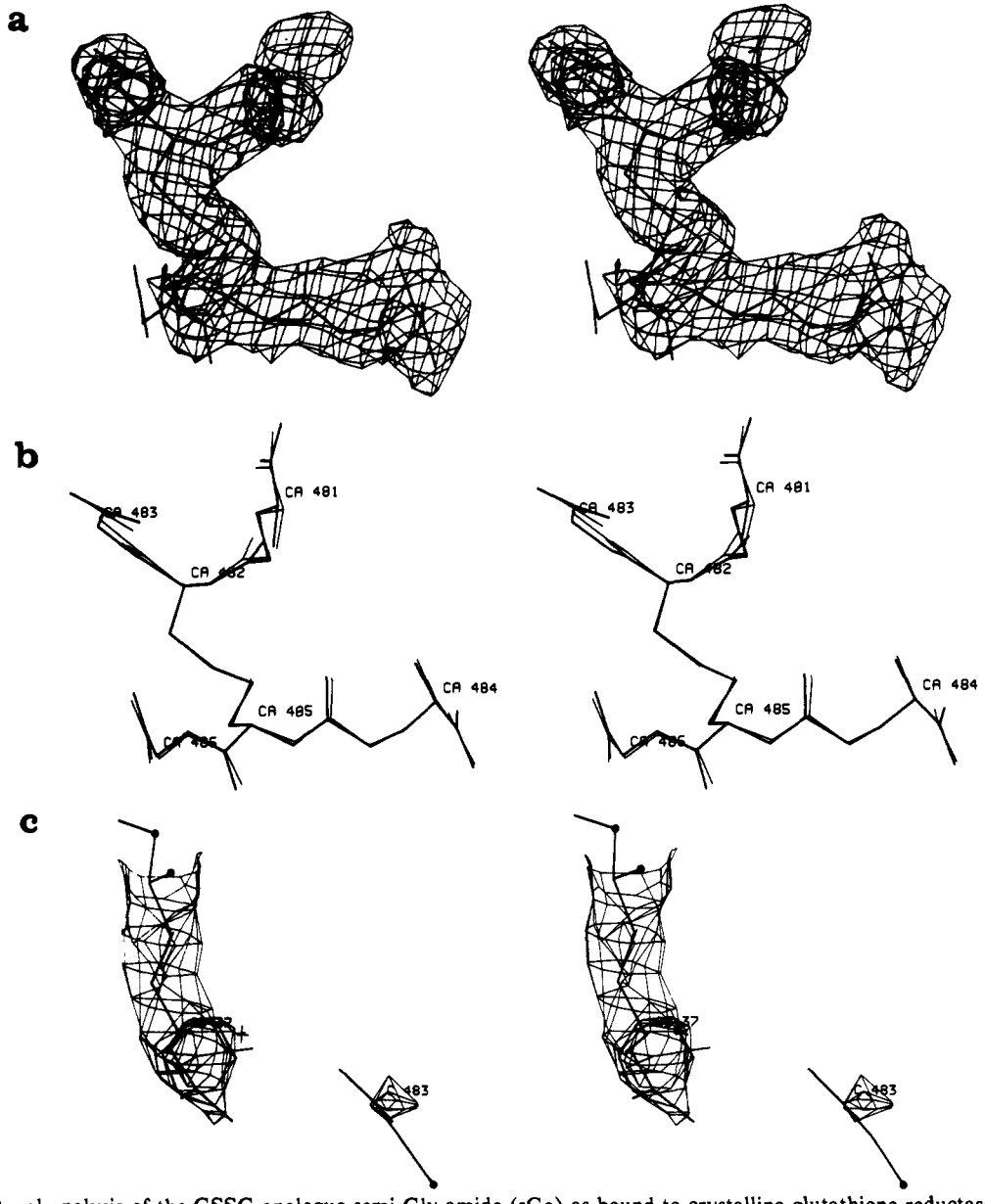

FIGURE 3: Structural analysis of the GSSG analogue semi-Gly-amide (sGa) as bound to crystalline glutathione reductase. (a) Difference Fourier electron density map with the refined model of sGa; the cut level is at 20% of maximum density (=2.3σ). (b) Overlay of the refined model of sGa (thick lines) with GSSG (thin lines, as in Figure 2b). (c) Additive Fourier electron density map ($2F_{soak} - F_{nat}$) exp$i\alpha_{calc}$ showing the refined models of Gly-I of sGa and Arg37 (thick lines). The cut level is at 15% of the maximum (=1.4σ). The native Arg37 conformation is given as thin lines. Chain cuts are marked by dots. The cross represents a solvent molecule.

contact partner of the carboxamide at Gly-I, remains in its native conformation (Figure 2c). In contrast, this guanidinium shifts by about 1 Å and rotates by about 20° on binding the respective carboxylate of GSSG. In other words, Arg37 welcomes an incoming carboxylate by moving to it, but remains reserved at its native place in the case of a carboxamide, forcing the latter in a conformation different from the carboxylate.

Binding of sGa. The difference density of sGa, which has only one of the glycines amidated, is given in Figure 3a. Following the geometry of bound GSSG, the model could be built easily into this density; the amide was placed at site Gly-II. After coordinate refinement, the resulting sGa model agreed within the limits of error with bound GSSG (Figure 3b). The additive Fourier in Figure 3c shows that the guanidinium group of Arg37 assumes a mixture of conformations, about 50% GSSG-like (contacting a carboxylate) and 50% native, which is bGa-like (contacting free solvent or a carboxamide).

The same conformation mixture of Arg37 is also observed with the bound analogues sEa and sdE that have definitely a carboxylate at Gly-I because none of the glycines is modified. The difference Fourier maps of sGa, sEa, and sdE have positive densities below the native guanidinium group position in Figure 3c that resemble each other closely but differ from the respective map of bGa. Therefore, we conclude that sGa is bound with its carboxylate at Gly-I and its amide at Gly-II. At Arg37, the difference between binding the carboxyl of sGa, sEa, or sdE on one hand and the carboxyl of GSSG on the other can be explained by occupancy differences. While the analogue occupancies range around 60% (see below), which leaves almost half the arginines in their native conformation, GSSG has about 100% occupancy (Karplus et al., 1989). In conclusion, the GSSG binding site accommodates a carboxamide at Gly-II rather than at Gly-I, so that sGa binds in single mode and not in a mixture of two modes.

Binding of sEa. The binding mode of sEa with one amidated glutamate carboxyl can be derived from the density map

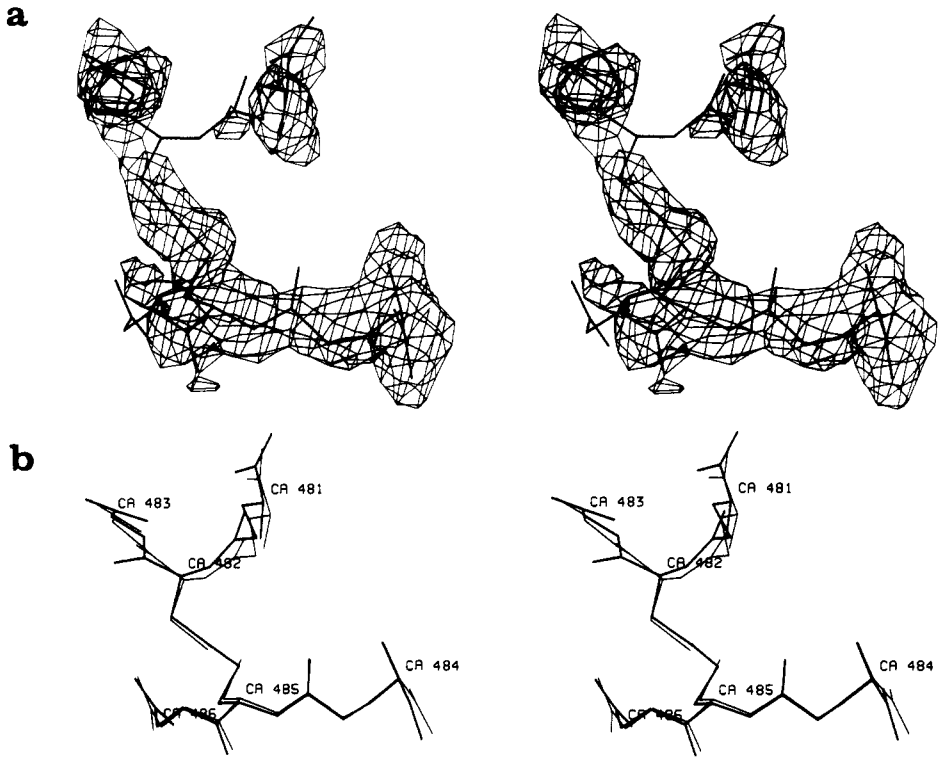

FIGURE 4: Structural analysis of the GSSG analogue semi-Glu-amide (sEa) as bound to crystalline glutathione reductase. (a) Difference Fourier electron density map with the refined model of sEa. The cut level is at 15% of the density maximum (=1.4σ), which is at Cys284. (b) Overlay of refined model of sEa (thick lines) with GSSG (thin lines, as in Figure 2b).

of Figure 4a. Here, Glu-I (and also Cys-I) has a much lower density than Glu-II, while for sGa, bGa, sdE, and GSSG, all of which have carboxylates at Glu-I and Glu-II, the respective densities are approximately equal. The density difference indicates strongly that sEa binds in a single mode, placing the amide modification at site Glu-I. The model was built accordingly. The conformation of the refined model is close to GSSG, except for Glu-I, where sEa shows a significant shift of 0.5–1 Å (Figure 4b).

Binding of sdE. Figure 5a shows the binding mode of sdE, which lacks one of the amino groups. In general, the density resembles the one of GSSG. But it shows clearly an amino group at Glu-II and no amino group at Glu-I, demonstrating that sdE binds in a single mode. The model was built accordingly with the deaminated glutamate at Glu-I. The model was refined, and the result was compared to GSSG as shown in Figure 5b. Although there occurred a change at Glu-I, the differences are within the limits of error and therefore not significant.

Most interestingly, however, the missing amino group induces a shift of catalytically competent residues as shown in Figure 5c. This shift seems to originate at the carboxylate of Glu472′, which among the shifted groups is nearest to the missing amino group [see Figure 6 and also Figure 5 of Karplus and Schulz (1989)]. The carboxylate rotates by about 30°, causing a movement of about 0.3 Å of the imidazole of His467′ together with the redoxactive disulfide Cys58:Cys63.

Occupancies. The relative occupancies of the ligands sGa, bGa, sEa, and sdE were determined by comparing the highest densities at Glu-II in the difference Fourier maps at 2.4-Å resolution. Glu-II was taken because all data show that it is generally least affected by substrate modifications. All occupanices are in a similar range (Table I).

In contrast, the absolute occupancies are more difficult to derive. The additive Fourier maps, which were calculated from $(2F_{soak} - F_{nat})\ \exp i\alpha_{calc} = (2(F_{soak} - F_{nat}) + F_{nat})\ \exp i\alpha_{calc}$, should give the densities of ligand and protein on the same scale, because a difference Fourier produces the ligand at half-scale (Blundell & Johnson, 1976). A comparison of the highest density of the disulfide of sGa, for example, with the redox active disulfide of the protein gives the ratio 0.3. With temperature factors around 10 Å^2 for the protein disulfide and around 30 Å^2 for the ligand disulfide (Karplus & Schulz, 1989), a density ratio of 0.3 converts to an absolute occupancy of $0.3(30/10)^{1/2} \cong 50\%$. Since the ligands have displaced several solvent molecules, these are always subtracted in our Fourier maps, shifting the absolute occupancy of sGa to somewhat higher values. Probably it is about 60%, which is appreciably lower than the absolute occupancy of 100% suggested for GSSG (Karplus et al., 1989). Considering the inaccuracies of the occupancy evaluation, we estimate that the absolute occupancies of the analogues range between 40% and 80%.

Enzyme Kinetics. The enzyme GR shows substrate inhibition for GSSG concentrations above about 1 mM (=11K_m, Table II). In contrast to GSSG, none of the analogues showed such inhibition in the concentration range examined here, which was maximally 5K_m. For all experiments we assumed Michaelis–Menten kinetics (Icēn, 1967) following the formula $v = V_{max}([S]/([S] + K_m))$. For the analogues with K_m values below 5 mM, the parameters V_{max} and K_m were derived from double-reciprocal plots (Table II). For the two analogues with higher K_m values, bEa and bdE, only the catalytic efficiencies V_{max}/K_m could be determined. This was done with direct linear plots. Here, we derived limits for V_{max} and K_m under the assumption that V_{max} is at least double the highest actually observed reaction rate v and at most the value for the respective analogue with single modification (sEa, sdE). The corresponding limits for K_m were calculated from the observed V_{max}/K_m. The solubilities and the available amounts of the GSSG analogues precluded the application of higher concentrations. For GSSG we determined V_{max} as 220 units/mg

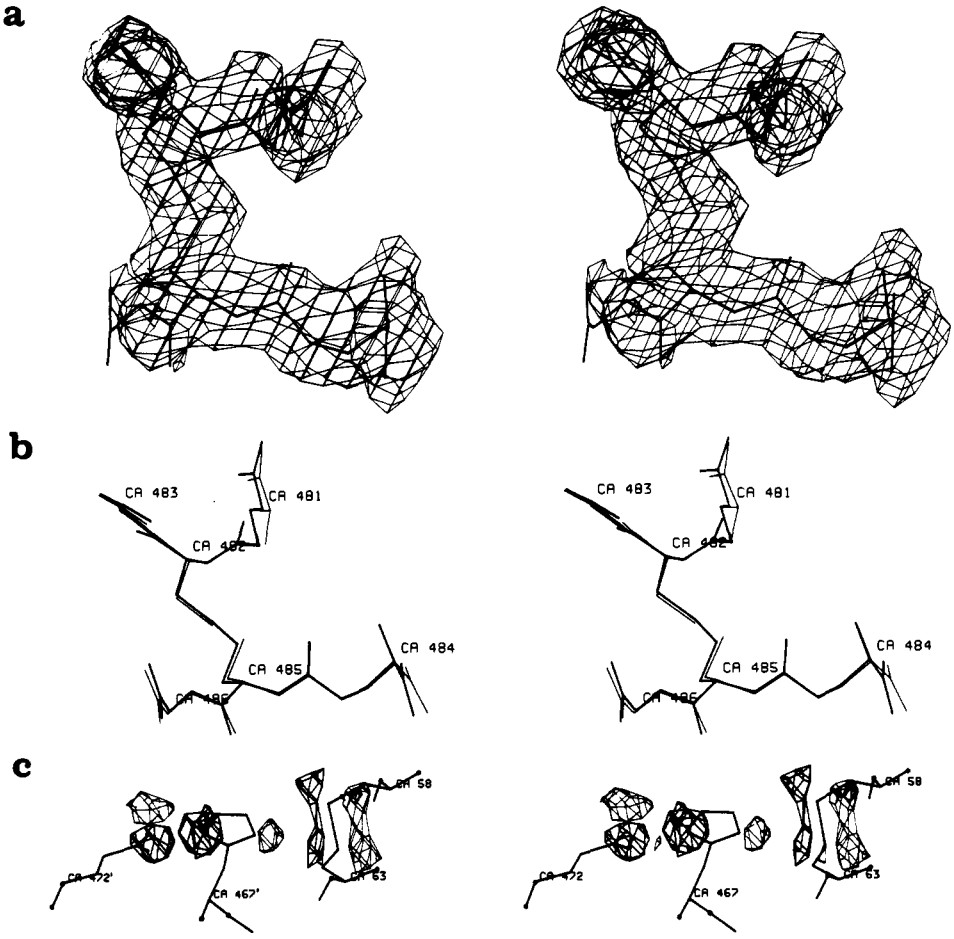

FIGURE 5: Structural analysis of the GSSG analogue semi-deamino-Glu (sdE) as bound to crystalline glutathione reductase. (a) Difference Fourier electron density map with the refined model of sdE; the cut level is at 20% of maximum density (=2.6σ). (b) Overlay of the refined model of sdE (thick lines) with GSSG (thin lines, as in Figure 2b). (c) Difference Fourier electron density map at the catalytic team consisting of the redox active disulfide Cys58:Cys63, His467′, and Glu472′. Positive (thick lines) and negative (thin lines) densities are given; the cut levels are at ±20% (=±2.6σ). The disulfide and the imidazole move from the right-hand side to the left.

in contrast to 240 units/mg observed by others (Worthington & Rosemeyer, 1974; Bilzer et al., 1984) under similar conditions; K_m was determined as 80 μM in contrast to 65 μM (Icên, 1967; Worthington & Rosemeyer, 1976; Bilzer et al., 1984).

The catalytic efficiencies V_{max}/K_m given in Table II lead to a clear ordering of the physiological substrate GSSG and its analogues. The same ordering applies for V_{max}, whereas the ordering of K_m is somewhat different (changes are marked by an asterisk):

V_{max}/K_m	GSSG > sGa > sEa > sdE > bGa > bEa > bdE
V_{max}	GSSG > sGa > sEa > sdE > bGa > bEa > bdE
K_m	GSSG < sGa < sdE* < sEa* < bGa < bdE* < bEa*

None of the analogues has better catalytic properties than GSSG. The analogues with a single modification (sGa, sEa, sdE) are in all respects closer to GSSG than those carrying two modifications (bGa, bEa, bdE).

Microcalorimetry. The amount of heat released on binding GSSG to GR was measured at five different temperatures. At full occupancy this is the binding enthalpy. The easily available substrate GSSG was used, because each measurement requires substantial amounts of the ligand, here, 55 mg of GSSG. Later experiments with GSSG analogues are planned. Assuming 100% occupancy, the binding enthalpies ΔH were −66, −103, −141, −188, and −219 kJ/mol at 20, 25, 30, 35, and 40 °C, respectively. All were measured twice; the scatter was about ±10 kJ/mol. These results lie well on a straight line with the slope −8 kJ·mol^{-1}·K^{-1}, which corresponds to the heat capacity change ΔC_p.

The actual occupancy can be calculated as $1/(1 + K_D/[GSSG])$ if the dissociation constant K_D is known. Since GR obeys Michaelis–Menten kinetics (Icên, 1967), a lower limit of the occupancy can be derived from the observed K_m as this is larger than K_D; $K_m = (k_{-1} + k_{cat})/k_{+1} \geq k_{-1}/k_{+1} = K_D$. The temperature dependence of K_D has to be taken into account. It was derived by integrating the van't Hoff formula $\partial \ln K_D/\partial T = -(\Delta H_{298} + \Delta C_p(T - 298))/RT^2$. With ΔH_{298} = −103 kJ/mol and ΔC_p = −8 kJ·mol^{-1}·K^{-1}, the change amounts to $K_{D,40°C}/K_{D,25°C} = 23$. Assuming $K_{D,25°C} = 50$ μM, which is reasonable as we found $K_{m,25°C} = 80$ μM (Table II) and others found 65 μM (see above), the occupancies at 25 and 40 °C are 99% and 86%, respectively. The occupancy decrease at higher temperatures causes no correction outside the limits of error stated below.

In conclusion, we find ΔH_{298} = −103 (±10) kJ/mol and ΔC_{p298} = −8 (±1) kJ·mol^{-1}·K^{-1} where the given errors are merely the scatter of the measurements. This ΔC_p value is higher than usual (Wiesinger & Hinz, 1986), but there exist other systems with ΔC_p in the same range (Wiesinger & Hinz, 1984; Gaudin et al., 1980). The experiments showed that ΔH and ΔC_p of GSSG analogues can be determined and that meaningful differences between the analogues may become available with careful measurements. It should be kept in mind, however, that the occupancies of the analogues have to be established accurately because they do not bind as well as

Table II: Enzyme Kinetics of the Physiological Substrate GSSG and Its Analogues

substrate	concn range (mM) min	max	enzyme[a] added (μg)	V_{max}/K_m[b] (%)	V_{max}[b] (%)	K_m (mM)	parameter ratios corresponding to individual contacts: contact	ratios[c] V_{max}/K_m	V_{max}	K_m	relation[c]
GSSG	0.02	3	0.13	100	100	0.08					
semi-Gly-amide (sGa)	0.02	2	0.13	18	87	0.42	Gly-II carboxylate	6	1.1	5	sGa vs GSSG
bis-Gly-amide (bGa)	0.05	5	1.3	1.2	33	2.3	Gly-I carboxylate	15	2.6	5	bGa vs sGa
semi-Glu-amide (sEa)	0.1	10	0.13	3.5	84	2.1	Glu-I carboxylate	29	1.2	25	sEa vs GSSG
bis-Glu-amide (bEa)	0.2	7	6.5	0.14	20–84	13–53	Glu-II carboxylate	25	4.2–1	6–25	bEa vs sEa
semi-deamino-Glu (sdE)	0.3	5	0.13	2.2	41	1.6	Glu-I amino	46	2.4	20	sdE vs GSSG
bis-deamino-Glu (bdE)	0.5	6	13	0.004	0.7–41	14–800	Glu-II amino	550	59–1	9–500	bdE vs sdE

[a] All enzyme concentrations were determined spectroscopically at 460 nm by using $\epsilon = 11\ mM^{-1}\ cm^{-1}$ per active site (Williams, 1976; Krauth-Siegel et al., 1985). The $\epsilon_{280}/\epsilon_{460}$ ratio was always 6, indicating 100% holoenzyme (Krohne-Ehrich et al., 1977). [b] All values are referred to those of GSSG and normalized to the amount of enzyme added for GSSG; V_{max} for GSSG is 220 units/mg. V_{max} and K_m are derived from double-reciprocal plots. The catalytic efficiencies V_{max}/K_m were derived from direct linear plots. [c] The K_m ratio refers to the given relation, whereas the V_{max} and the V_{max}/K_m ratios are inverted; for instance, the K_m ratio of contact Glu-I carboxylate (sEa vs GSSG) is $25 \cong 2.1/0.08$, while the corresponding V_{max} ratio is $1.2 \cong 100/84$.

GSSG (see K_m in Table II) and because limited solubilities prevent a substantial increase of enzyme and/or ligand concentrations. This can only be achieved with radioactive labels, rendering organic synthesis more difficult.

Discussion

In our X-ray studies we analyzed the binding modes of four GSSG analogues (sGa, bGa, sEa, sdE); one analogue (bdE) was scarcely visible and one (bEa) not visible at all. The absolute occupancies of sGa, bGa, sEa, and sdE range between 40% and 80% (see above), which is in reasonable agreement with the K_m values of Table II if we consider K_m as similar to the dissociation constant K_D. For bEa and bdE, the low occupancies correlate with the high K_m values. It should be noted that the K_m values were measured at physiological conditions, whereas the occupancies were observed at high salt concentrations in the crystal. However, the error introduced by the ionic strength difference should remain in an acceptable range, as the enzyme is still active with similar catalytic parameters at crystal conditions. For GSSG at crystal conditions, Bilzer et al. (1984) found $V_{max} = 200$ units/mg (83% with respect to physiological conditions) and $K_m = 90\ \mu M$ (=140%). Considering $K_m = 90\ \mu M$ in the crystal, a 10 mM soak of GSSG should result in more than 99% occupancy ($K_D \leq K_m$), which agrees with an estimate from X-ray analysis (Karplus et al., 1989).

For evaluating the effect of substrate modifications on binding and processing, one has to make sure that the analogue binds in a single mode, which is not always the case (Karplus et al., 1989), and that it binds as expected, which cannot be taken for granted (Christianson et al., 1989). For example, the analogue *S*-(2,4-dinitrophenyl)glutathione attached to GR with its intact glutathione moiety binding to neither one of the two glutathione sites (Bilzer et al., 1984). In our analysis, all six GSSG analogues showed catalytic activity so that binding similarity can be expected. The four structurally analyzed analogues had conformations very similar to GSSG. Still, the semiderivatized GSSG analogues sGa, sEa, and sdE may bind in two alternative modes. Single-mode binding will only occur if the Gibbs free energy differences between the alternative contact disturbances are large enough.

The binding contacts of GSSG with GR are sketched in Figure 6. Three of the six charged substrate groups form direct salt bridges. The other three charged substrate groups form salt bridges only via solvent molecules (Figure 6). The GSSG analogues synthesized here have either one or two charges removed. For sEa, the density maps showed clearly single-mode binding with the amide at Glu-I (Figure 4a). This

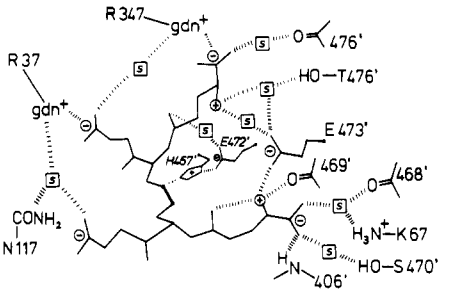

FIGURE 6: Sketch of the contacts between the charged groups of GSSG and the protein, as based on the structure of the complex GR/GSSG that had been refined at 2-Å resolution (Karplus & Schulz, 1989). Contact mediating solvent molecules (s) are included. Hydrogen bonds are indicated by hashed bonds. The residues are given in one-letter-code whenever side chains are involved in the interactions. Primed residue numbers belong to the other subunit of the dimeric enzyme. The view corresponds approximately to Figures 2–5. The disulfide and its interaction with imidazole are marked.

demonstrates that the carboxyl at Glu-I (direct salt bridge) is less important for binding than the carboxyl at Glu-II (indirect salt bridge).

Also, sdE was bound in single mode (Figure 5a). Since the missing amino group is at Glu-I, we conclude that, with respect to binding, the amino group at Glu-I (indirect salt bridge) is less important than the amino group at Glu-II (direct salt bridge). The analysis of analogue sGa is complicated by the movement of Arg37 (Figure 3). It is clearly indicated, however, that there occurs single-mode binding with the amide at Gly-II (indirect salt bridge) and not at Gly-I (direct salt bridge), which agrees with the very low density at Gly-II found for all ligands. Scoring direct and indirect salt bridges indicates that direct bridges are not decisively stronger than indirect ones.

Since bEa and bdE have catalytic activity (Table II), they do bind to the enzyme, though weakly. For bdE, which has both amino groups removed, the observed low density at Glu-II and Cys-II demonstrates that a missing amino group at Glu-II does not abolish binding. Since the densities of Figures 2a, 3a, 4a, and 5a show in accordance with previous work (Karplus et al., 1989) that Glu-II is the most strongly bound part of GSSG, the residual affinity of deaminated Glu-II in bdE and the even lower affinity of amidated Glu-II in bEa points to a major role of the Glu-II carboxyl in binding.

Since the X-ray data of four GSSG analogues show localized contact changes and since this scheme can be extended to the other two analogues (Table II), we can relate these local differences to the changes of catalytic parameters. For ranking, we equate the ratios V_{max}/K_m, V_{max}, and K_m for

substrates without and with contact modification to the respective contact contributions. These ratios are given at the right-hand side of Table II. This is only a rough estimate, as noncooperative addition of the contributions is assumed; i.e., a second disturbance (e.g., bGa vs sGa) is treated like an initial one (sGa vs GSSG). For simplicity, we consider K_m to correspond to binding, while V_{max} gives the catalytic rate k_{cat} of the bound ligand.

The smallest drop of V_{max}/K_m (factor of 6) is caused by amidation at Gly-II (sGa vs GSSG), which essentially affects binding (K_m) only; the V_{max} ratio is 1.1, and the K_m ratio is 5 (Table II). In contrast, the amide at Gly-I (bGa vs sGa) leads to a larger drop in V_{max}/K_m (factor of 15); it affects binding as well as catalysis. Here, the reduction of k_{cat} could have been caused, for instance, by a 0.3-Å shift of the essential atom Cys-I-S, which would evade our detection.

The next largest drops of V_{max}/K_m occur on amidation at Glu-I and Glu-II. The decrease at Glu-I (sEa vs GSSG) is essentially caused by diminished binding (K_m), while k_{cat} drops only marginally. At Glu-II (bEa vs sEa) it was not possible to distinguish between binding and catalysis. Zero occupancy in the crystal together with the affinity difference between Glu-I and Glu-II as indicated by single-mode binding (Figure 4a), however, points to a large binding effect (K_m ratio close to 25). It is conceivable that amidation affects the strong hydrogen bond to Met406′-N appreciably (Figure 6).

The most dramatic reduction of catalytic efficiency occurs on amino group removal. As judged from Figure 6, the amino group at Glu-I (sdE) does not seem important, as it forms no direct contact to the protein. Still, its removal causes a very large drop in V_{max}/K_m (factor of 46) mostly related to diminished binding (K_m). Moreover, sdE has the lowest k_{cat} among the analogues with a single modification. This can be explained by the observed shift of the catalytically competent residues Glu472′, His467′, and Cys58:Cys63 as shown in Figure 5c. This shift is most likely a consequence of the positive amino charge missing in a central area of the local charge arrangement consisting of His467′, Glu472′, Glu473′, Glu-I, and Glu-II.

For the double derivative bdE, the positive amino charge of Glu-II is removed from the central area of this arrangement in addition to the one of Glu-I. V_{max}/K_m decreased to very low values (factor of 550, see Table II) so that V_{max} and K_m could not be determined separately. There is residual binding as we do see part of the ligand in the crystal, indicating that the K_m value is probably not too far away from the lower limit of 14 mM. We therefore conclude that the removal of the second amino group reduces the catalytic rate most dramatically.

This is in agreement with the difference Fourier map of bdE, which in addition to low occupancy at Cys-II and Glu-II showed essentially the same shift of the catalytically competent residues Glu472′ and His467′ as the singly modified derivative sdE, i.e., a carboxyl rotation by about 30° together with a imidazole shift toward Glu472′ of about 0.3 Å. In contrast to sdE, however, there occurs no shift of the redox active disulfide Cys58:Cys63 so that the catalytically competent team is taken apart, abolishing catalysis almost completely. Since the difference Fourier map reports the change vs the unliganded enzyme, this dissruption requires not only the absence of the substrate amino groups but also the presence of the Cys-II and/or Glu-II moieties of the substrate that are visible and therefore bound in the crystal.

It should be noted that if the assumptions "$K_m = K_D$" and "additivity" (e.g., bGa vs sGa treated like sGa vs GSSG) were exactly correct, the K_m ratios for the amide at Gly-I and at Gly-II, for example, would reflect the respective Gibbs free energy contributions. Since these K_m ratios are both 5 (Table II), there should be no preference, and sGa should bind in mixed mode with the amide evenly distributed over Gly-I and Gly-II, which is not the case. Essentially the same situation is observed for the amidations and deaminations of Glu (see Table II). As a consequence, the assumptions merely provide guidelines, but do not allow far-reaching conclusions. In particular, the assumed additivity has to be checked by analyzing further combinations of modifications.

In conclusion, the presented data allow a differential diagnosis of the GSSG site of GR with respect to charges and a distinction between changes in binding and in processing of the substrate. The discrepancy between observation and expectation is most spectacular for the amino groups, the removal of which demonstrated that GR catalyzes the correct substrate not only by selecting for optimal binding strength and geometry but also by making catalytic competent residues like His467′ and Glu472′ sensitive to substrate modifications. In GR this is presumably achieved by incorporating these two amino acids as well as the substrate amino groups in a fragile charge cluster, which breaks down, abolishing catalysis if essential components are incorrect.

ACKNOWLEDGMENTS

We thank Dr. P. A. Karplus and U. Ermler for discussions and Dr. A. Blume for allowing us to use his microcalorimeter.

REFERENCES

Baker, E. N., & Hubbard, R. E. (1984) *Prog. Biophys. Mol. Biol. 44*, 97–179.

Bilzer, M., Krauth-Siegel, R. L., Schirmer, R. H., Akerboom, T. P. M., Sies, H., & Schulz, G. E. (1984) *Eur. J. Biochem. 138*, 373–378.

Blundell, T. L., & Johnson, L. N. (1976) *Protein crystallography*, p 407, Academic Press, New York.

Christianson, D. W., Mangani, S., Shoham, G., & Lipscomb, W. N. (1989) *J. Biol. Chem. 264*, 12849–12853.

Dolphin, D., Poulson, R., & Avramovic, O., Eds. (1989) *Glutathione*, Wiley, New York.

Gaudin, C., Marty, B., Ragot, M., Sari, J. C., & Belaich, J. P. (1980) *Biochimie 62*, 741–746.

Hol, W. G. J. (1986) *Angew. Chem., Int. Ed. Engl. 25*, 767–778.

Holden, H. M., & Matthews, B. W. (1988) *J. Biol. Chem. 263*, 3256–3260.

Icēn, A. L. (1967) *Scand. J. Clin. Lab. Invest. Suppl. 96*, 1–67.

Jones, T. A. (1978) *J. Appl. Crystallogr. 11*, 268–272.

Karplus, P. A., & Schulz, G. E. (1987) *J. Mol. Biol. 195*, 701–729.

Karplus, P. A., & Schulz, G. E. (1989) *J. Mol. Biol. 210*, 163–180.

Karplus, P. A., Pai, E. F., & Schulz, G. E. (1989) *Eur. J. Biochem. 178*, 693–703.

Krauth-Siegel, R. L., Schirmer, R. H., & Ghisla, S. (1985) *Eur. J. Biochem. 148*, 335–344.

Krohne-Ehrich, G., Schirmer, R. H., & Untucht-Grau, R. (1977) *Eur. J. Biochem. 80*, 65–71.

Scheuring, J. (1988) Diploma thesis, Universität Freiburg i. Br.

Schirmer, R. H., Krauth-Siegel, R. L., & Schulz, G. E. (1989) in *Glutathione* (Dolphin, D., Poulson, R., & Avramovic, O.,

Eds.) pp 553–596, Wiley, New York.
Sustmann, R., Sicking, W., & Schulz, G. E. (1989) *Angew. Chem., Int. Ed. Engl. 28*, 1023–1025.
Thieme, R., Pai, E. F., Schirmer, R. H., & Schulz, G. E. (1981) *J. Mol. Biol. 152*, 763–782.
Tronrud, D. E., TenEyck, L. F., & Matthews, B. W. (1987) *Acta Crystallogr. A43*, 489–501.
Wieland, T., & Sieber, A. (1969) *Liebigs Ann. Chem. 727*, 121–124.
Wiesinger, H., & Hinz, H.-J. (1984) *Biochemistry 23*, 4921–4928.
Wiesinger, H., & Hinz, H.-J. (1986) in *Thermodynamic Data for Biochemistry and Biotechnology* (Hinz, H.-J., Ed.) pp 211–226, Springer-Verlag, Heidelberg.
Williams, A. P. (1986) *J. Chromatogr. 373*, 175–190.
Williams, C. H., Jr. (1976) *Enzymes (3rd Ed.) 13*, 89–173.
Worthington, D. J., & Rosemeyer, M. A. (1974) *Eur. J. Biochem. 48*, 167–177.
Worthington, D. J., & Rosemeyer, M. A. (1976) *Eur. J. Biochem. 67*, 231–238.

CORRECTION

Two-Step Internalization of Ca^{2+} from a Single $E\sim P\cdot Ca_2$ Species by the Ca^{2+}-ATPase, by Daniel Khananshvili and William P. Jencks*, Volume 27, Number 8, April 19, 1988, pages 2943–2952.

We and our colleagues A. M. Hanel and T. Fujimori have been unable to prepare vesicles and carry out experiments that confirm the results reported in Figures 2 and 3. Therefore, the experimental results and conclusions reported in this paper must be withdrawn pending further experimental examination. We deeply regret the necessity for this correction.